POLAR SPIN AXIS ANOMALY

Patrick L. Crouse ,Thomas W. Flatley, and Wendy M. Morgenstern
Goddard Space Flight Center (GSFC)
Greenbelt, Maryland

Abstract

The Global Geospace Science (GGS) Polar Plasma Laboratory (POLAR) spacecraft was launched on February 24, 1996, by a Delta II. The spacecraft, a major axis spinner, appeared to function nominally throughout the early mission phase, which included several deployments, and orbit and attitude maneuvers. Of particular interest is the fact that the spacecraft was launched with a deliberate dynamic imbalance. During a segment of early orbit operations, a pair of Lanyard Deployed Booms (LDB) were extended. These booms were not identical; the intent was that the spacecraft would be nearly dynamically balanced after they were deployed. The spacecraft contained two dynamic balance mechanisms intended to fine tune the balance on orbit. However, subsequent images taken by the science instruments on the Despun Platform during the dynamic balancing segment indicated an offset of the principal spin axis from the geometric axis. This offset produced a sinusoidal blurring of the science images sufficiently large to degrade science data below mission requirement specifications. In the end, the imbalance encountered in flight was significantly outside the correction capability of the balances. The purpose of this paper is to examine the flight data during the various deployment and maneuver stages of the early orbit operations coupled with analytical simulations to discuss some of the potential causes of the resultant imbalance.

INTRODUCTION

The Polar Plasma Laboratory (POLAR) spacecraft was launched on February 24, 1996, by a Delta II. The spacecraft, a major axis spinner, appeared to function nominally throughout the early mission phase, which included several deployments, and orbit and attitude maneuvers. The spacecraft was launched with a deliberate dynamic unbalance, i.e., with intentional products of inertia. During early orbit operations, a pair of Lanyard Deployed Booms (LDB) were extended. These booms were not identical; the intent was that the spacecraft would be nearly dynamically balanced after they were deployed. The spacecraft contained two dynamic balance mechanisms intended to fine tune the balance on orbit. However, subsequent images taken by the science instruments on the Despun Platform during the dynamic balancing segment indicated an offset of the principal spin axis from the geometric axis. This offset produced a sinusoidal blurring of the science images sufficiently large to degrade science data below mission requirement specifications. In the end, the imbalance encountered in flight was significantly outside the correction capability of the balances. The purpose of this paper is to examine the flight data during the various deployment and maneuver stages of the early orbit operations coupled with analytical simulations to discuss some of the potential causes of the resultant imbalance. These findings are compared and contrasted with those of the spacecraft manufacturer.

MISSION OVERVIEW AND SPACECRAFT DESCRIPTION

The GGS program is part of the overall International Solar Terrestrial Physics (ISTP) program designed to use multiple spacecraft in complementary orbits to assess processes in the Sun-Earth interaction chain. The GGS program uses POLAR and its sister spacecraft, the Interplanetary Physics Laboratory (WIND)

launched in November 1994, to specifically investigate the solar wind-magnetosphere coupling and the global magnetosphere energy transport. These phenomena include solar wind source and 3-D features, global plasma storage flow and transformation, deposition of energy into the atmosphere, and basic plasma states and characteristics. Both spacecraft were constructed by Lockheed Martin Corporation (formerly the Astrospace Division of General Electric) to be spin stabilized cylindrical spacecraft about 2.44 meters in diameter and 1.85 meters tall. The mission orbit for POLAR is 1.8 X 9.0 Earth Radii (Re) at an inclination of 86°, with the apogee over the North Pole to maximize auroral imaging.

The POLAR spacecraft, shown in Figure 1, has eight science instruments mounted on the spinning main body, and four imaging instruments on the despun platform on the +Z end of the spacecraft. Appendages include four 65-m radial wire antennas, two 6-m long spin axis antenna booms, a search coil, loop antenna, and two 6-m long lanyard deployed booms (LDB). The LDBs are truss-like structures canted downward from the spin plane by 3.5°, and deployed in the +/-X directions with the Magnetic Field Experiment (MFE) instrument on the +X and the Plasma Wave Investigation (PWI) instrument on the -X sides. The four radial wire antennas, referred to as +/-U and +/-V wires, and the six propellant tanks (not shown) are located in the center of gravity (CG) plane to minimize effects of any uncertainties in wire length and fuel distribution on spacecraft balance[1]. In the normal mission mode, POLAR orients the spin axis within 1° of the positive or negative orbit normal vector, and maintains a spin rate of 10 rpm. The selection of $\pm$ orbit normal is based on a Sun angle constraint of 90° to 160° from the +Z-axis due to power and thermal needs.

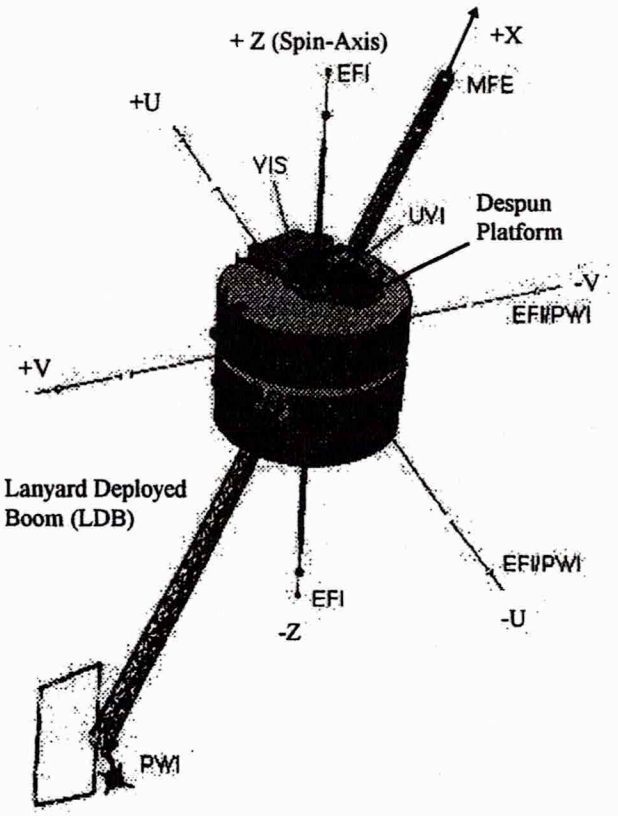

Figure 1: POLAR Spacecraft

OVERVIEW OF ANOMALY

The attitude sensors on the POLAR spacecraft are positioned so that they do not provide observation of a spin-axis offset from the principal axis. The data gathered from a series of propulsive maneuvers, and appendage deployments over the launch and early orbit (L&EO) portion of the mission indicated that the mission was proceeding nominally. During despun platform activation sequence, it was pointed to a selected star which would appear as essentially a single pixel in the instrument field of view. By taking multiple images over time, a spin axis offset would manifest itself as a sinusoidal blurring of the pixel image. The images taken during this dynamic balancing segment indicated an offset of the principal spin axis from the geometric axis of 0.26°, an order of magnitude greater than the 0.02° mission requirement. The pre-launch analysis performed by the spacecraft manufacturer indicated a worst case offset of 0.095° in the XZ plane, and 0.18° in the YZ plane[1]. The dynamic balancer masses were sized accordingly, and constrained as part of a trade study of mass versus propellant reserves. Further study of the on-flight dynamic balancing data revealed that the offset was at a phase angle of 195° which meant it was near the plane of the LDBs, which is the XZ plane. In terms of the products of inertia, the observed offset was approximately three times larger than the worst case analysis, and twice as large as the compensation capability of the balancer[1]. Additionally, movement of the balancers did not produce the predicted change in spin axis offset. Next, the dynamics of the spinning spacecraft at various stages of deployment is examined.

ANALYSIS

The Euler equations of motion are applied to the spacecraft rigid core. The effects of the hydrazine fuel and the wires are included as external torques acting on the core. We will consider only the steady state conditions. Figure 2 illustrates how the torque due to a typical flexible element is computed. Each of the six hydrazine fuel tanks, and the four wires can be characterized as a point mass, m, at a distance ℓ from an attach point, which is at a distance a from the spin axis. All the attach points and the system center of mass are in a plane normal to the nominal spin axis.

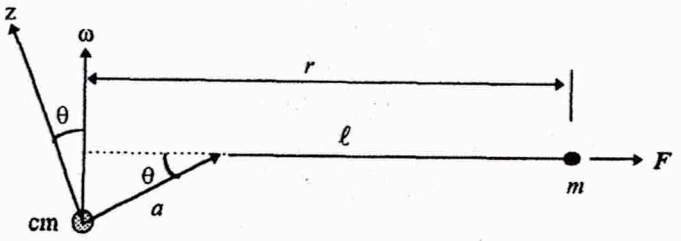

Figure 2: Torque Due to a Flexible Element

The magnitude of the torque due to the forces acting on the elemental mass is

$$T = Fa\sin\theta = ma(a\cos\theta + \ell)\omega^2 \sin\theta$$

The direction of the torque is given by

$$\hat{t} = \frac{\vec{\omega} \times \vec{a}}{a\omega\cos\theta}$$

So the torque vector, $\vec{T}$, is exactly

$$\vec{T} = T\hat{t} = \frac{m\sin\theta(a\cos\theta + \ell)\omega}{\cos\theta}\vec{\omega} \times \vec{a}$$

Assuming that θ is small, then

$$\vec{T} \approx m\sin\theta(a+\ell)\omega\vec{\omega}\times\vec{a} = \frac{m(a+\ell)\vec{\omega}\cdot\vec{a}\vec{\omega}\times\vec{a}}{a}$$

The Six Hydrazine Tanks

The values of m, a and ℓ are the same for each tank. Let $\vec{a}_i$ be a vector from the system center of mass to the center of a typical tank and let $\vec{\omega}$ be the spacecraft angular velocity vector. Let $\vec{a}_0$ be located at an arbitrary azimuth angle (ϕ) away from the +x-axis. The torque generated by each tank is

$$\vec{T}_i = m\,\frac{(a+\ell)}{a}\,\vec{\omega}\cdot\vec{a}_i\vec{\omega}\times\vec{a}_i$$

Table 1: Location of Center of Each Tank

Tank Number	Azimuth Angle	Tank Center Coordinates		
		a_x	a_y	a_z
0	ϕ	$a\cos(\phi)$	$a\sin(\phi)$	0
1	$\phi + \pi/3$	$a\cos(\phi+\pi/3)$	$a\sin(\phi+\pi/3)$	0
2	$\phi + 2\pi/3$	$-a\sin(\phi+\pi/6)$	$a\cos(\phi+\pi/6)$	0
3	$\phi + \pi$	$-a\cos(\phi)$	$-a\sin(\phi)$	0
4	$\phi + 4\pi/3$	$a\sin(\phi-\pi/6)$	$-a\cos(\phi-\pi/6)$	0
5	$\phi + 5\pi/3$	$a\sin(\phi+\pi/6)$	$-a\cos(\phi+\pi/6)$	0

Using the information provided in Table 1, the components of the torque found due to all the tanks is:

$$T_x = -3ma(a+\ell)\,\omega_z\,\omega_y$$
$$T_y = 3ma(a+\ell)\,\omega_z\,\omega_x$$
$$T_z = 0$$

Note that this result is independent of the initial phase angle (ϕ). In general, for any number of symmetrically placed tanks n greater than 2, the component torque is

$$T_x = -\frac{n}{2}ma(a+\ell)\,\omega_z\,\omega_y$$
$$T_y = \frac{n}{2}ma(a+\ell)\,\omega_z\,\omega_x$$
$$T_z = 0$$

The POLAR fuel tank radius is 11.00 in., and the distance from the spin axis to the center of the tanks is 25.10 in. The propellant density is 0.0364 lb/in^3. The remaining fuel in the propellant system is estimated to be 90.16 kg usable and 5.7 kg non-usable for a total of 95.86 kg. Assume that each tank contains 15 kg of hydrazine which contributes to the attenuation of the dynamic imbalance. The location of the center of mass of the hydrazine fuel in a tank is illustrated in Figure 3. To solve for ℓ, we have to compute the location of the center of mass of the remaining fuel. The incremental mass, dm, and the incremental mass moment are found as

$$dm = \rho\pi(r^2 - x^2)dx$$
$$dM = xdm$$

and

$$\ell = \frac{M}{m}$$

Now,

$$m = \rho\pi \int_{x_0}^{r} (r^2 - x^2)dx = \rho\pi \left[r^2 x - \frac{x^3}{3} \right]_{x_0}^{r} = 15\text{kg}$$

MACSYMA was used to obtain $x_0 = 5.37655$ in. Then the mass moment is

$$M = \rho\pi \int_{x_0}^{r} x(r^2 - x^2)dx = \rho\pi \left[\frac{r^2 x^2}{2} - \frac{x^4}{4} \right]_{x_0}^{r} = 242.461$$

Then, $\ell = 7.35$ inches (or 0.19 m), and thus, $ma(a + \ell) = 8\text{kg} \cdot \text{m}^2$.

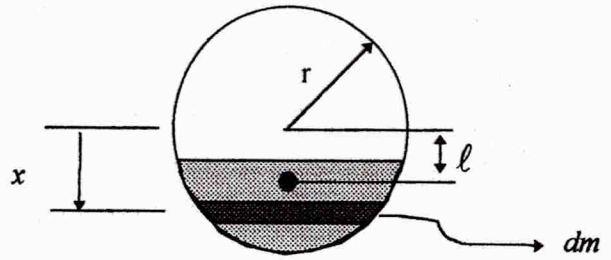

Figure 3: Location of Center of Mass of Hydrazine in Tank

The torques contributing to the dynamic imbalance attenuation are:

$$T_x = -24\omega_z\omega_y$$
$$T_y = 24\omega_z\omega_x$$
$$T_z = 0$$

Prior to the deployment of the LDBs or the wires the spacecraft moment of inertia tensor was, by design,

$$I = \begin{bmatrix} 816.80 & 10.02 & -0.69 \\ 10.02 & 685.40 & 0.31 \\ -0.69 & 0.31 & 830.50 \end{bmatrix}$$

The steady state spin axis associated with the above tensor may be found approximately by considering the first two equations arising from the condition $\vec{\omega} \times \vec{H} = 0$, where $\vec{H} = I\vec{\omega}$ is the spacecraft angular momentum vector. This relationship may be expressed by:

$$\begin{bmatrix} 0 & -\omega_z & \omega_y \\ \omega_z & 0 & -\omega_x \\ -\omega_y & \omega_x & 0 \end{bmatrix} \begin{bmatrix} 816.80 & 10.02 & -0.69 \\ 10.02 & 685.40 & 0.31 \\ -0.69 & 0.31 & 830.50 \end{bmatrix} \begin{bmatrix} \omega_x \\ \omega_y \\ \omega_z \end{bmatrix}$$

Linearized in ω_x and ω_y, the first two equations are given by:

$$10.02\ \omega_x - 145.1\ \omega_y = -0.31\ \omega_z$$
$$13.7\ \omega_x - 10.02\ \omega_y = -0.69\ \omega_z$$

Solving these equations for ω_x/ω_z and ω_y/ω_z yields

$$\omega_x/\omega_z = -0.0514$$
$$\omega_y/\omega_z = -0.00141$$

This represents a tilt of about 3°, almost completely in the -x direction.

If we include the influence of the fuel, the equation of interest becomes:

$$\begin{bmatrix} 0 & -\omega_z & \omega_y \\ \omega_z & 0 & -\omega_x \\ -\omega_y & \omega_x & 0 \end{bmatrix} \begin{bmatrix} 816.80 & 10.02 & -0.69 \\ 10.02 & 685.40 & 0.31 \\ -0.69 & 0.31 & 830.50 \end{bmatrix} \begin{bmatrix} \omega_x \\ \omega_y \\ \omega_z \end{bmatrix} = \begin{bmatrix} -24\omega_y\omega_z \\ 24\omega_x\omega_z \\ 0 \end{bmatrix}$$

Again linearizing in ω_x and ω_y, the first two equations become

$$10.02\ \omega_x - 169.1\ \omega_y = -0.31\ \omega_z$$
$$37.7\ \omega_x - 10.02\ \omega_y = -0.69\ \omega_z$$

The solution to these equations is

$$\omega_x/\omega_z = -0.0181$$
$$\omega_y/\omega_z = 0.0008$$

This represents a 1° degree tilt in the -x direction, so the fuel has attenuated the dynamic imbalance by a factor of three.

The Wires

Recall that the torques due to the wires are given by

$$\vec{T} = \frac{m(a+\ell)}{a}\vec{\omega}\cdot\vec{a}\vec{\omega}\times\vec{a}$$

where the $\vec{a}$ vectors locate the roots of the deployed wires. There are two U-wires, deployed to the same length, nominally extending radially outward from the spin axis in the first and third quadrants of the XY plane. Likewise, a pair of V-wires are deployed in the second and fourth quadrants. The component torques due to the U-wires are given by

$$T_{x_u} = -m_u a(a+\ell_u)(\omega_x+\omega_y)\omega_z$$
$$T_{y_u} = m_u a(a+\ell_u)(\omega_x+\omega_y)\omega_z$$

where m_u is the mass and ℓ_u is the length of the deployed portion of the U-wires. The torques due to the V-wires are

$$T_{x_v} = m_v a(a+\ell_v)(\omega_x-\omega_y)\omega_z$$
$$T_{y_v} = m_v a(a+\ell_v)(\omega_x-\omega_y)\omega_z$$

For all wires, a = 1.19 meters. The first deployment was that of the U-wires, which were simultaneously deployed to a length of 20 meters. The mass of wire deployed was 0.395 kg and the wire center of mass was 14.96 meters from the root.

This produced the torques:

$$T_x = -7.59(\omega_x + \omega_y)\omega_z$$
$$T_y = 7.59(\omega_x + \omega_y)\omega_z$$

The rigid core mass properties changed slightly, and the equilibrium equations become:

$$\begin{bmatrix} 0 & -\omega_z & \omega_y \\ \omega_z & 0 & -\omega_x \\ -\omega_y & \omega_x & 0 \end{bmatrix} \begin{bmatrix} 816.20 & 10.60 & -0.69 \\ 10.60 & 684.80 & 0.31 \\ -0.69 & 0.31 & 829.30 \end{bmatrix} \begin{bmatrix} \omega_x \\ \omega_y \\ \omega_z \end{bmatrix} = \begin{bmatrix} -24\omega_y\omega_z - 7.59(\omega_x + \omega_y)\omega_z \\ 24\omega_x\omega_z + 7.59(\omega_x + \omega_y)\omega_z \\ 0 + \text{second order terms} \end{bmatrix}$$

The solution of these equations is

$$\omega_x/\omega_z = -0.01534$$
$$\omega_y/\omega_z = 0.00150$$

Spin Axis Determination in Symbolic Form

Now consider the spin axis determination. The rigid core moment of inertia tensor is given by

$$I = \begin{bmatrix} I_{xx} & -I_{xy} & -I_{xz} \\ -I_{xy} & I_{yy} & -I_{yz} \\ -I_{xz} & -I_{yz} & I_{zz} \end{bmatrix}$$

Let the rigid core angular velocity vector be given by

$$\vec{\omega} = \begin{bmatrix} \omega_x \\ \omega_y \\ \omega_z \end{bmatrix}$$

The Euler Equations of Motion for the rigid core are

$$I\frac{d\vec{\omega}}{dt} + \vec{\omega} \times I\vec{\omega} = \vec{T}$$

where $\vec{T}$ is the external torque vector. At equilibrium, or steady state rotation, $\vec{\omega}$ is a constant, therefore

$$\begin{bmatrix} 0 & -\omega_z & \omega_y \\ \omega_z & 0 & -\omega_x \\ -\omega_y & \omega_x & 0 \end{bmatrix} \begin{bmatrix} I_{xx}\omega_x - I_{xy}\omega_y - I_{xz}\omega_z \\ -I_{xy}\omega_x + I_{yy}\omega_y - I_{yz}\omega_z \\ -I_{xz}\omega_x - I_{yz}\omega_y + I_{zz}\omega_z \end{bmatrix} = \begin{bmatrix} T_x \\ T_y \\ T_z \end{bmatrix}$$

Expanding further, with ω_x and ω_y considered small, the first two linearized equations become

$$-\omega_z(-I_{xy}\omega_x + I_{yy}\omega_y - I_{yz}\omega_z) + \omega_y(I_{zz}\omega_z) = T_x$$
$$\omega_z(I_{xx}\omega_x - I_{xy}\omega_y - I_{xz}\omega_z) - \omega_x(I_{zz}\omega_z) = T_y$$

or

$$I_{xy}\omega_x + (I_{zz} - I_{yy})\omega_y = T_x - I_{yz}\omega_z$$
$$(I_{xx} - I_{zz})\omega_x - I_{xy}\omega_y = T_y + I_{xz}\omega_z$$

or, if we decompose the external torque into fuel and wire components,

$$I_{xy}\omega_x + (I_{zz} - I_{yy})\omega_y = T_{x_f} + T_{x_u} + T_{x_v} - I_{yz}\omega_z$$
$$(I_{xx} - I_{zz})\omega_x - I_{xy}\omega_y = T_{y_f} + T_{y_u} + T_{y_v} + I_{xz}\omega_z$$

Let $k_f = 3ma(a+\ell)$, then the torque due to the fuel is

$$T_{x_f} = -k_f\omega_z\omega_y$$
$$T_{y_f} = k_f\omega_z\omega_x$$

The equations then become

$$I_{xy}\omega_x + (I_{zz} - I_{yy} + k_f\omega_z)\omega_y = T_{x_u} + T_{x_v} - I_{yz}\omega_z$$
$$(I_{xx} - I_{zz} - k_f\omega_z)\omega_x - I_{xy}\omega_y = T_{y_u} + T_{y_v} + I_{xz}\omega_z$$

If we let $k_u = m_u a(a+\ell_u)$ and $k_v = m_v a(a+\ell_v)$, and substitute for the torques, then

$$\left[I_{xy} + (k_u - k_v)\right]\frac{\omega_x}{\omega_z} + \left[(I_{zz} - I_{yy}) + (k_f + k_u + k_v)\right]\frac{\omega_y}{\omega_z} = -I_{yz}$$
$$\left[(I_{xx} - I_{zz}) - (k_f + k_u + k_v)\right]\frac{\omega_x}{\omega_z} - \left[I_{xy} + (k_u - k_v)\right]\frac{\omega_y}{\omega_z} = I_{xz}$$

These are simultaneous equations with ω_x/ω_z and ω_y/ω_z as unknowns which may be solved to find the body rates ratios.

Sun Angle Change

The Sun aspect angle at the time of the first deployment was approximately 95.3° and it changed by +0.12° during the deployment. This is the angle between the geometric z-axis and the Sun vector, measured once per spin by a slit Sun sensor 65° away from the +x-axis in the direction of the +y-axis. Let θ be the measured angle. The Sun vector in body coordinates at the time the angle is measured is given by

$$S_x = \sin(\theta)\cos(65)$$
$$S_y = \sin(\theta)\sin(65)$$
$$S_z = \cos(\theta)$$

Flight data shows that the fuel and the deployed wires constitute an extremely effective nutation damper. The spacecraft also contains a fluid-filled loop passive damper. The consequence of this damping is that

the angular velocity vector (in addition to the angular momentum vector) remains inertially fixed during the deployment. Since the Sun vector is also nearly inertially fixed, we can calculate a predicted Sun angle change during the deployment by assuming that $\vec{\omega} \cdot \vec{S}$ is constant.

From results given above, before deployment we have ω_x/ω_z = - 0.0181 and ω_y/ω_z = 0.0008, and a Sun angle of 95.3°. After deployment, we have ω_x/ω_z = - 0.01534 and ω_y/ω_z = 0.0015 and we let the Sun angle be 95.3 + q degrees.

$$\left.\frac{\vec{\omega} \cdot \vec{S}}{\omega_z}\right|_{\text{Pre-deploy}} = -0.0181 \sin(95.3)\cos(65) + 0.008 \sin(95.3)\sin(65) + \cos(95.3)$$

$$\left.\frac{\vec{\omega} \cdot \vec{S}}{\omega_z}\right|_{\text{Post-deploy}} = -0.01534 \sin(95.3+q)\cos(65) + 0.0015 \sin(95.3+q)\sin(65) + \cos(95.3+q)$$

Equating these two dot products and solving for q, we find q = 0.10° compared to a measured change of 0.12° or 17% lower.

Sun Angle Change in Symbolic Form

As previously noted, when the Sun passes through the Sun sensor field of view, the Sun unit vector has the components

$$S_x = \sin(\theta)\cos(65)$$
$$S_y = \sin(\theta)\sin(65)$$
$$S_z = \cos(\theta)$$

After a configuration change, assume that the new Sun vector is given by

$$S_x' = \sin(\theta)\cos(65)$$
$$S_y' = \sin(\theta)\sin(65)$$
$$S_z' = \cos(\theta)$$

Assume that the Sun angle change is q, i.e. let $\theta = \theta + q$. Then, using the trigonometric identity,

$$\sin(\theta') = \sin(\theta)\cos(q) + \cos(\theta)\sin(q)$$
$$\cos(\theta') = \cos(\theta)\cos(q) - \sin(\theta)\sin(q)$$

For q<<1, we have the approximations

$$\sin(\theta') = \sin(\theta) + q\cos(\theta)$$
$$\cos(\theta') = \cos(\theta) - q\sin(\theta)$$

and

$$S_x' = \left[\sin(\theta) + q\cos(\theta)\right]\cos(65)$$
$$S_y' = \left[\sin(\theta) + q\cos(\theta)\right]\sin(65)$$
$$S_z' = \cos(\theta) - q\sin(\theta)$$

Now, let the initial angular velocity vector be given by [ω_x,ω_y,1] and the new angular velocity vector by [ω_x',ω_y',1]. For $\vec{\omega} \cdot \vec{S}$ constant, we have

$$\frac{\omega_x}{\omega_z}S_x+\frac{\omega_y}{\omega_z}S_y+S_z=\frac{\omega_x'}{\omega_z}S_x'+\frac{\omega_y'}{\omega_z}S_y'+S_z'$$

or

$$\frac{\omega_x}{\omega_z}\sin\theta\cos 65+\frac{\omega_y}{\omega_z}\sin\theta\sin 65+\cos\theta=\frac{\omega_x'}{\omega_z}(\sin\theta+q\cos\theta)\cos 65+\frac{\omega_y'}{\omega_z}(\sin\theta+q\cos\theta)\sin 65-q\sin\theta$$

This equation may be solved for q, the Sun angle change

$$q=\frac{\sin\theta\left[\cos 65\left(\frac{\omega_x}{\omega_z}-\frac{\omega_x'}{\omega_z}\right)+\sin 65\left(\frac{\omega_y}{\omega_z}-\frac{\omega_y'}{\omega_z}\right)\right]}{\cos\theta\left(\frac{\omega_x'}{\omega_z}\cos 65+\frac{\omega_y'}{\omega_z}\sin 65\right)-\sin\theta}$$

Substituting in the numbers presented above and solving i.e., ωx/ωz = - 0.0181, ωy/ωz = 0.0008, ωx'/ωz = - 0.01534 and ωy'/ωz = 0.0015 and θ = 95.3 degrees, we find that q = 0.0018 radians or 0.10°.

<u>Products of Inertia Determined by Sun Angle Changes</u>

Suppose that the critical products of inertia I_{xz} and I_{yz} are treated as unknowns, while all the other moment of inertia tensor elements are known. All wire deployments are symmetrical and do not change these products. Consider now a wire deployment event for which a Sun angle change is measured, such as the one just described above. There are five equations involved, and all parameters are known except for the two products of inertia:

$$\Rightarrow \quad \left[I_{xy}+(k_u-k_v)\right]\frac{\omega_x}{\omega_z}+\left[(I_{zz}-I_{yy})+(k_f+k_u+k_v)\right]\frac{\omega_y}{\omega_z}=-I_{yz}$$

$$\Rightarrow \quad \left[(I_{xx}-I_{zz})-(k_f+k_u+k_v)\right]\frac{\omega_x}{\omega_z}-\left[I_{xy}+(k_u-k_v)\right]\frac{\omega_y}{\omega_z}=I_{xz}$$

$$\Rightarrow \quad \left[I_{xy}'+(k_u'-k_v')\right]\frac{\omega_x'}{\omega_z'}+\left[(I_{zz}'-I_{yy}')+(k_f'+k_u'+k_v')\right]\frac{\omega_y'}{\omega_z'}=-I_{yz}$$

$$\Rightarrow \quad \left[(I_{xx}'-I_{zz}')-(k_f'+k_u'+k_v')\right]\frac{\omega_x'}{\omega_z'}-\left[I_{xy}'+(k_u'-k_v')\right]\frac{\omega_y'}{\omega_z'}=I_{xz}$$

$$\Rightarrow \quad q=\frac{\sin\theta\left[\cos 65\left(\frac{\omega_x}{\omega_z}-\frac{\omega_x'}{\omega_z}\right)+\sin 65\left(\frac{\omega_y}{\omega_z}-\frac{\omega_y'}{\omega_z}\right)\right]}{\cos\theta\left(\frac{\omega_x'}{\omega_z}\cos 65+\frac{\omega_y'}{\omega_z}\sin 65\right)-\sin\theta}$$

Combining these equations yields a constraint on the products I_{xz} and I_{yz}. An equation of the form

$$AI_{xz}+BI_{yz}=C$$

where A, B and C are known constants. There are two movable masses on the spacecraft, intended to fine tune the rigid core products of inertia, I_{xz} and I_{yz}, ideally to zero. Dynamic Balancer No. 1 (DB_1) is located at x = - 0.33 m and y =1.01 m. DB_2 is located at x = -1.01 m and y = - 0.33 m. The range of motion is +/- 0.51 m (20 in.). The DB_1 mass weighs 2.56 kg, so its adjustment capability is $I_{xz} = 0.43\text{kg}\cdot\text{m}^2$ and $I_{yz} = 1.32\text{kg}\cdot\text{m}^2$. The mass of DB_2 is 2.74 kg, and the capability to affect the products of inertia is $I_{xz} = 1.41\text{kg}\cdot\text{m}^2$ and $I_{yz} = 0.46\text{kg}\cdot\text{m}^2$.

Tables 2-4 illustrate the 17 major deployment events, in addition to spin, spin axis attitude, and orbit maneuvers, that occurred during the first 34 days. Table 2 contains the spacecraft dry core inertias, while Table 3 shows the values for k_f, k_u, and k_v at each stage. Table 4 shows the measured Sun angle at each stage, as well as both the observed and predicted change in Sun angle as a result of the event. The predicted change is calculated following the analysis outlined above. The search coil deploy (event 5), the lanyard deployed boom (8), the despun platform activation (14), and the movement of dynamic balancer number 2 (15) are of particular interest. The difference between the observed Sun angle change, and the predicted change for these events are about 3 to 5 times greater than the other events. The next step then was to examine the flight data more closely in search of infomation that went unnoticed during this operations period.

LAUNCH AND EARLY ORBIT REVIEW

The following sections are based on observed data during mission operations, and are described in greater detail in both Reference 1 and 2. The initial on-orbit assessment of the spacecraft shortly after launch indicated that a nominal injection had occurred. The measured spin rate was 48.1 rpm and the Sun angle was 60.7°, and the expected values were 48.2 rpm and 60.3°, respectively. Immediately, a maneuver planned to move the spacecraft to a thermal- and power-safe attitude was initiated, but one thruster failed. A backup maneuver plan was prepared, and the maneuver was completed. The Sun angle measured was 96.3°, when the target had been 95.0°. The differences in what was achieved versus what was expected was not an issue at the time, due to the large degree of uncertainty in injection attitude, and thruster performance, and the large operating range that was deemed acceptable.

Table 2: Dry Core Moments of Inertias for Deployment Phases

	Configuration	Corresponding Dry Core Inertias (kg-m^2)					
		I_{xx}	I_{yy}	I_{zz}	I_{xy}	I_{xz}	I_{yz}
1	**Pre-Deployment**	816.800	685.400	830.500	-10.020	0.690	-0.310
2	**U-Wires to 20 m**	816.200	684.800	829.300	-10.600	0.690	-0.310
3	**V-Wires to 20 m**	815.600	684.200	828.200	-10.020	0.690	-0.310
4	**Loop Antenna Deploy**	815.500	685.100	828.900	-10.050	0.870	-0.220
5	**Search Coil Deploy**	815.100	685.500	829.700	-9.990	0.670	-0.280
6	**Hat Jettison**	815.100	685.500	829.700	-9.990	0.670	-0.280
7	**U-Wires to 35 m**	814.900	685.300	829.300	-10.160	0.670	-0.280
8	**LDB Deployment**	822.500	1338.300	1474.900	-11.990	0.150	-0.150
9	**V-Wires to 35 m**	822.300	1338.100	1474.600	-11.820	0.150	-0.150
10	**U-Wires to 50 m**	822.100	1338.000	1474.300	-11.990	0.150	-0.150
11	**V-Wires to 50 m**	821.900	1337.800	1473.900	-11.820	0.150	-0.150
12	**U-Wires to 65 m**	821.800	1337.600	1473.600	-11.990	0.150	-0.150
13	**Z Boom Deployment**	865.600	1381.400	1473.600	-11.990	0.150	-0.150
14	**DSP Activation**	861.400	1385.600	1445.900	-12.100	0.040	0.030
15	**DB2 +17.5 inches**	861.941	1386.140	1445.900	-12.100	-1.187	-0.372
16	**DB2 +2.5 inches**	862.106	1386.310	1445.900	-12.100	-1.362	-0.429
17	**DB1 +8.6 inches**	862.229	1386.430	1445.900	-12.100	-1.547	0.134

Table 3: Values of k_f, k_u, and k_v for Various Deployment Phases

	Configuration	Fuel in each tank (kg)	Wire Lengths		k_f	k_u	k_v
			U-wire lengths (m)	V-wire lengths (m)			
1	Pre-Deployment	15.0	0.0	0.0	26.4	0.0	0.0
2	U-Wires to 20 m	15.0	20.0	0.0	26.4	7.6	0.0
3	V-Wires to 20 m	15.0	20.0	20.0	26.4	7.6	7.6
4	Loop Antenna Deploy	15.0	20.0	20.0	26.4	7.6	7.6
5	Search Coil Deploy	15.0	20.0	20.0	26.4	7.6	7.6
6	Hat Jettison	15.0	20.0	20.0	26.3	5.9	5.9
7	U-Wires to 35 m	15.0	35.0	20.0	26.3	13.0	5.9
8	LDB Deployment	15.0	35.0	20.0	26.3	13.0	5.9
9	V-Wires to 35 m	15.0	35.0	35.0	25.8	13.0	13.0
10	U-Wires to 50 m	15.0	50.0	35.0	25.8	22.4	13.0
11	V-Wires to 50 m	15.0	50.0	50.0	25.6	22.4	22.4
12	U-Wires to 65 m	15.0	65.0	50.0	25.6	34.1	22.4
13	Z Boom Deployment	15.0	65.0	50.0	25.6	34.1	22.4
14	DSP Activation	15.0	65.0	50.0	25.5	34.1	22.4
15	DB2 +17.5 inches	15.0	65.0	50.0	25.5	34.1	22.4
16	DB2 +2.5 inches	15.0	65.0	50.0	25.5	34.1	22.4
17	DB1 +8.6 inches	15.0	65.0	50.0	25.5	34.1	22.4

Table 4: Calculation of Spin Axis Offset and ΔSun Angle versus ΔObserved Sun Angle

	Configuration	Spin Axis Tilt By Calculation		Approximate Sun Angle (deg)	ΔObserved Sun Angle (deg)	ΔCalculated Sun Angle (deg)
		Amplitude (deg)	Phase (deg)			
1	Pre-Deployment	0.975348	177.258749	0.0000	0.0000	0.0000
2	U-Wires to 20 m	0.83842	174.15018	95.3000	0.1200	0.095175
3	V-Wires to 20 m	0.721361	175.477407	95.5100	0.0300	0.023154
4	Loop Antenna Deploy	0.903309	178.792525	96.4000	-0.1200	-0.110832
5	Search Coil Deploy	0.676216	175.751944	96.2800	0.1600	0.123519
6	Hat Jettison	0.721346	176.139059	97.6000	-0.0300	-0.022636
7	U-Wires to 35 m	0.645191	173.380901	97.7700	0.0700	0.058443
8	LDB Deployment	0.048471	104.321606	98.4000	0.3000	0.243308
9	V-Wires to 35 m	0.046379	104.296719	127.8500	-0.0100	-0.001606
10	U-Wires to 50 m	0.044977	105.33082	127.7600	0.0100	-0.001605
11	V-Wires to 50 m	0.042498	105.318298	125.2900	-0.0150	-0.001886
12	U-Wires to 65 m	0.041092	106.540249	125.2100	0.0100	-0.001646
13	Z Boom Deployment	0.050834	104.162574	123.5000	0.005	0.008656
14	DSP Activation	0.012568	-105.907236	121.7000	-0.0900	-0.051855
15	DB2 +17.5 inches	0.181985	55.835873	110.0000	0.2500	0.199719
16	DB2 +2.5 inches	0.209727	55.994845	109.0000	0.0400	0.027476
17	DB1 +8.6 inches	0.143644	-22.06278	108.0000	-0.2200	-0.199709

Search Coil and Lanyard Deployed Boom Deployments

The deployment of the PWI Search Coil was not a big event from a flight dynamics perspective, considering that the primary concern at the time was spacecraft spin rate maintenance, and this event was to produce a negligible change in spin rate. The loop antenna failed to latch properly initially, and bounced against its stops. It did latch up during a subsequent spin up maneuver, and is behaving nominally. The observed change in the Sun angle did match well with simulations performed by the spacecraft manufacturer[1]. In addition, the spacecraft was nutating at the time of the deploy, which makes the observed data less reliable.

The lanyard deployed boom (LDB) sequence appears to be more interesting. At the time, the LDB deploy seemed nominal, mainly because it produced the expected final spacecraft spin rate, and the critical criteria for operations was for the booms to deploy at the same rate. Looking closer, there is an unexpected simultaneous change in both the Sun angle, and the accelerometer measurement about two minutes into the deployment. Plots of both the Sun angle, and the accelerometer data are presented in Figures 4 and 5. Review of WIND data, which also had LDB deployments, showed no such signature. However, steady-state values of the Sun angle following the maneuver indicate a nominal change in spin axis location as a result of this deploy.

Two other data transients are seen in both the Sun and accelerometer data at 12 and 30 hours following the deployment. The 18 hour difference constitutes a single orbit. These times are coincident with orbit perigee crossing, and it was believed it was due to gravity gradient effects. But in a deployed state, the effects should theoretically only produce about 0.01° change with no hysteresis[3]. This compares well with the observed values of 0.02°. However, between the transients, there is a constant migration of the spin axis that amounts to about 0.1-0.23°. The Magnetic Field Experiment (MFE) also measured a change in the angle between the magnetic x-axis and the spacecraft spin axis of about 0.35°. Subsequent analysis indicated that if the LDB failed, the MFE would always measure a larger angle than that calculated for the spacecraft body. The information suggests that the LDB suffered a permanent deformation, which has caused a significant change in spacecraft mass properties[1].

Despun Platform Activation and Dynamic Balancing

The despun platform was activated following pyro firing. Review of this activation suggests that the firing would have caused a large mechanical disturbance to both booms, and may have caused a shift in either non-rigid boom1. However, the disturbance should not have caused the LDB to fail, and does not explain the events mentioned above. The platform was stepped up to 10 rpm to despin it from the spacecraft main body, transmitting momentum to the spacecraft and spinning it up slightly as expected. The FDD calculated the platform pointing (not spin axis) to be about 0.2° from that done onboard the satellite, but the discrepancy was attributed to imbalances, and decreased significantly following the first round of dynamic balancing. During dynamic balancing, the spin axis did not move as expected for the commanded balance mass movement. This is further indication of a change in spacecraft mass properties from what was expected.

CONCLUSIONS

A change in mass properties from those expected have caused the POLAR spin axis offset. The reason for the mass properties change is less clear. The spacecraft manufacturer, as detailed in Reference 1, performed a complete analysis of the failure scenarios, and identified some possibilities. Pre-launch analysis was reviewed, and no errors were discovered, although final spacecraft close out activities did introduce some uncertainties. Masses at the ends of the LDB had the right magnitude to cause the imbalance. Review of the procedures showed the proper weight installed, but photos do not definitively

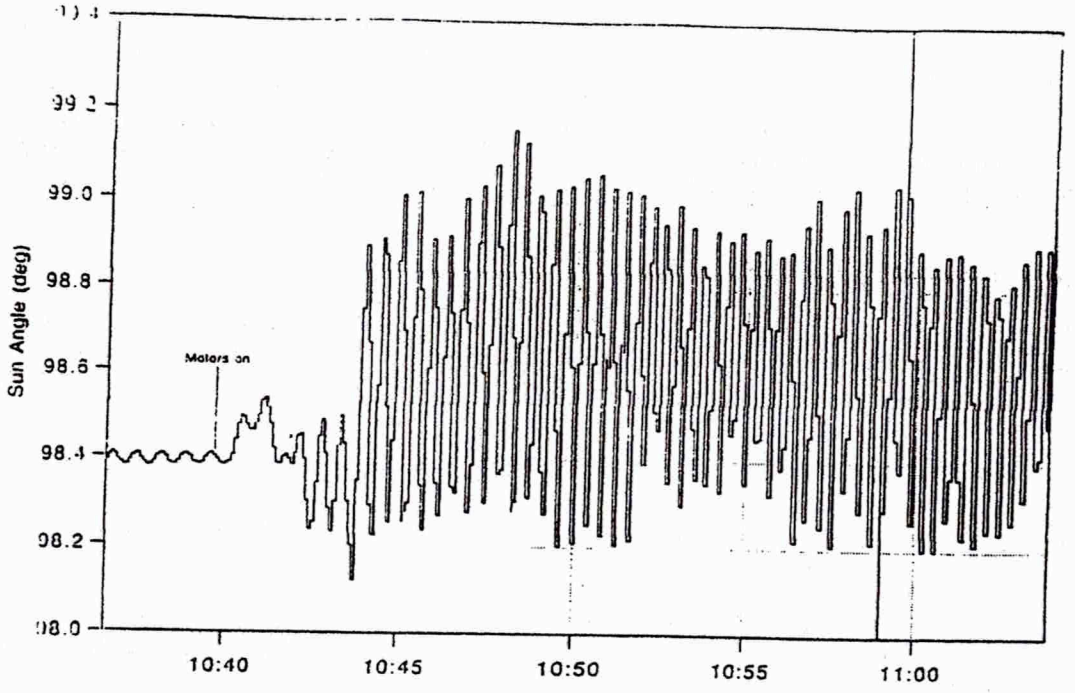

Figure 4: Lanyard Boom Deployment Sun Angle Data

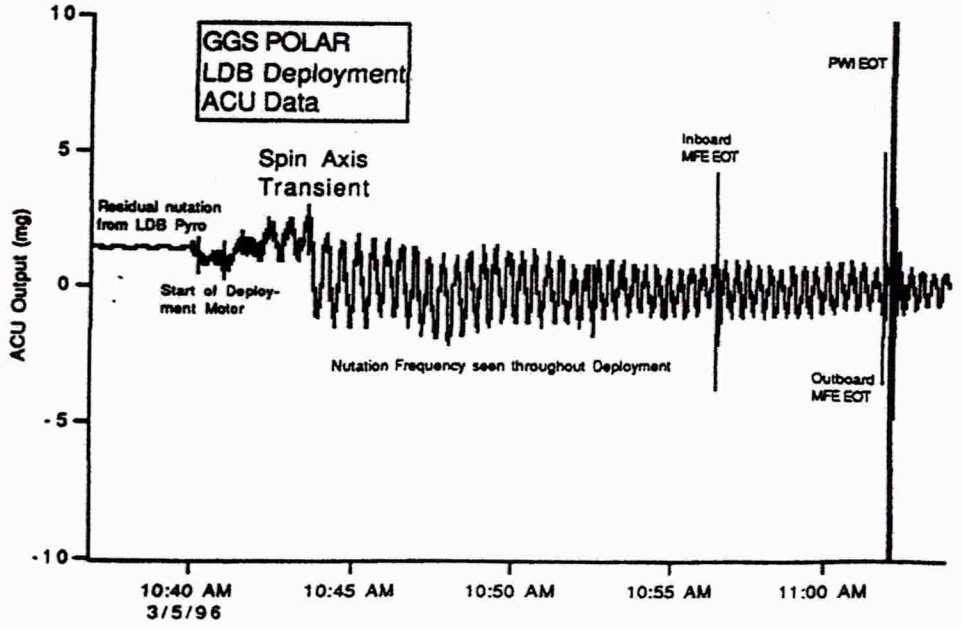

Figure 5: Lanyard Boom Deployment Accelerometer Data

show the masses as present since they would have been beneath a thermal blanket. Since the spin axis offset is in the plane of the LDB, and there is evidence of anomalous behavior during and after the deployment, the LDBs are the most likely cause of the imbalance. The properties are such that a 0.5° misalignment of one boom, or 0.25° of both booms, would cause the observed offset. While we may never know for sure, the authors share this conclusion with the spacecraft manufacturer. One positive note to make about this anomaly is that since the blurring of the science data is such a well defined pattern, post-processing software is able to recover the measurements for scientific analysis.

ACKNOWLEDGMENTS

The authors would like to thank Keith Baranoff from Lockheed Martin for his help in this investigation of the anomaly and his review of the paper. Keith has detailed knowledge of the dynamics of the spacecraft, and his assistance and knowledge have been greatly appreciated.

REFERENCES

1. Lockheed Martin Missiles and Space, "POLAR Spin Axis Anomaly Summary Report", CDRL 226, Contract No. NAS5-30503, August 19, 1996.

2. Goddard Space Flight Center, Flight Dynamics Division, 553-FDD-96/006R0UD0, *Interplanetary Physics Laboratory (WIND) and Polar Plasma Laboratory (POLAR) Postlaunch Report*, J.Dibble, July 1996.

3. Tom Flatley, GSFC, Notes, Summer 1996.